Hindawi
Adsorption Science & Technology
Volume 2022, Article ID 1267460, 13 pages
https://doi.org/10.1155/2022/1267460

Research Article

Optimization by Box–Behnken Design and Synthesis of Magnetite Nanoparticles for Removal of the Antibiotic from an Aqueous Phase

Marjan Salari

Department of Civil Engineering, Sirjan University of Technology, Sirjan, Iran

Correspondence should be addressed to Marjan Salari; salari.marjan@gmail.com

Received 8 October 2021; Revised 11 January 2022; Accepted 31 March 2022; Published 27 April 2022

Academic Editor: Gaurav Sharma

Some environmental problems caused by the intrusion of active drug ingredients, especially antibiotics, into water resources pose a serious threat. Ciprofloxacin (CIP) is an antibiotic from the group of fluoroquinolones that is used extensively in the treatment of bacterial infections. The presence of drug residues in the environment, especially in water resources, is an essential issue due to their stability and nondegradability. This study is aimed at investigating the efficiency of magnetite (Fe_3O_4) nanoparticles and the effect of independent variables, including initial concentrations of CIP (35-80 mg/L), adsorbent doses (20–60 mg), and pH values (4–10) at reaction time (80 min) for the removal efficiency of CIP antibiotics based on the Box-Behnken design (BBD) method. The analysis of variance (ANOVA) results indicated that a quadratic model was convenient for modeling CIP removal. The first step, the coprecipitation method, was appropriate for the preparation of Fe_3O_4 nanoparticles and developed as highly efficient adsorbents. Synthesized nanoparticles were later characterized by X-ray diffraction (XRD), Scanning Electron Microscopy (SEM), and Fourier transform infrared spectra (FT-IR). The results of XRD have shown that angles for the peaks at $2\theta = 30, 35.22, 43.35, 53.68, 57, 62.79,$ and 71.38 deg, which corresponded to the crystal planes 220, 311, 400, 422, 511, 440, and 535, respectively, were consistent with standard peaks of magnetite and a cubic face structure. The obtained results indicated that the CIP removal efficiency was 74.44% under optimum operation parameters: initial concentration of CIP 44.15 (mg/L), adsorbent dosage of 59.6 (mg), pH ≅ 5, and contact time of 80 min. In fact, a cooperative agreement between model prediction and experimental data using BBD with significant R^2 values of 0.95 was observed. Based on the results, magnetite nanoparticles have an excellent ability to remove antibiotics from an aqueous phase.

1. Introduction

Water is a natural and essential resource for human survival, and that is why human beings have always been looking for clean and healthy water for life. Various methods were carried out to evaluate the quality of surface water and groundwater [1–6]. Today, freshwater resources are endangered due to increased population growth and climate change [7–10]. The slow decomposition and incomplete metabolism of antibiotics have shown that more than 95% of it is not metabolized and goes into wastewater, making it more stable in the environment and polluting surface water and groundwater [11]. Antibiotics, with domestic wastewater, medicinal effluents, hospital wastewater, veterinary clinics, and agricultural products significantly enter the water resource and environment [12]. Antibiotic resistance is one of the main reasons for the purification of antibiotics, which may cause significant threats to global human health [13]. One of the prominent antibiotic families is fluoroquinolones that can be mentioned as ciprofloxacin (CIP), norfloxacin (NOR), and ofloxacin (OFL), which are widely used in therapeutic fields [13–15]. The presence of fluorine atoms in the composition of these antibiotics causes their stability and is considered stable and nonbiodegradable in the environment [15, 16]. CIPs are extensively used to treat bacterial infections (urinary tract infections) [17–19]. They have been detected in wastewater and surface water at concentrations of less than 1 μg/L, in

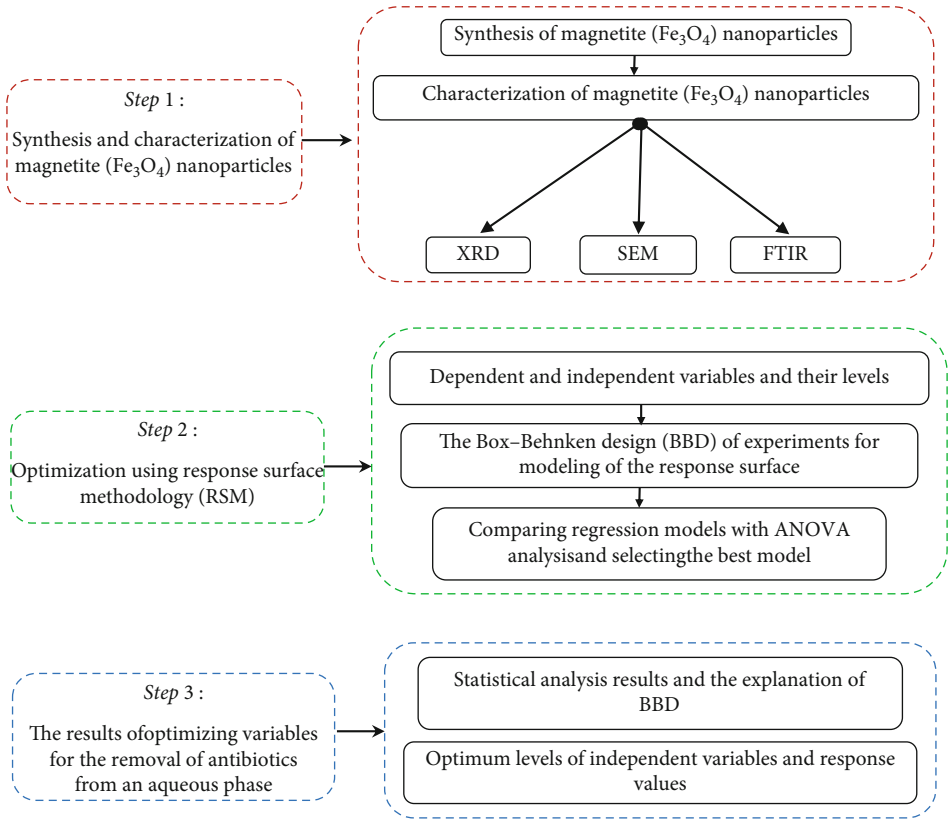

Figure 1: The proposed methodology for optimization of CIP removal by synthesis of magnetite (Fe_3O_4) nanoparticles using BBD.

hospital effluents at concentrations of above 150 μg/L, and in pharmaceutical plants at concentrations of about 30 mg/L [12]. Besides, the antibiotics can also be absorbed in the sludge at 2.43 mg/kg [12]. To remove contaminants, various studies through physical, chemical, biological, and combined methods have been used [20–22]. The results of these studies showed that most of these methods have not been cost-effective, due to the inability to completely decompose contaminants and the high cost of investment, as well as low returns, complex management and maintenance, and lengthy time [23–27]. Due to the indiscriminate and arbitrary use of antibiotics and the impossibility of removing these compounds by standard processes in municipal, hospital, and pharmaceutical wastewater treatment plants, the study of practical and feasible methods is inevitable [12].

Among the mentioned methods, adsorption processes are good options for separation due to their simplicity, low operating cost, low energy consumption, high flexibility, and the availability of numerous cheap adsorbents with complex properties. Adsorption is a type of separation operation similar to the liquid adsorption process in terms of the shape of the mass transfer operation. In the adsorption process, some of the soluble components in the fluid phase are transferred to the active surface of the solid adsorbent. The reason for using this process is the appropriate selectivity of the adsorbent to adsorb one or more components of the carrier fluid. The adsorption involves the accumulation of adsorbed molecules on the inner and outer surfaces of the adsorbent. Porous adsorbents with a high surface-area-to-volume ratio are usually common for possible utilization [27–30]. Nowadays, nanotechnologies in water and wastewater treatment have been developed using materials and processes such as zerovalent iron (nZVI) and magnetite (Fe_3O_4) nanoparticles [31–34].

Table 1: Selected levels of independent variables in BBD.

Influencing factors	-1	0	+1
Initial concentration of CIP (mg/L)	35	57.5	80
Adsorbent dose (mg)	20	40	60
pH (-)	4	7	10

In a study, researchers examined cephalexin (CEX) to be removed from an aqueous solution by powdered activated carbon coated with ZnO and nZVI nanoparticles derived from pomegranate peel extract. This study showed that the promotion of nanoparticles in the form of composites could be applied, and biophilic adsorbents remove CEX from an aqueous solution [34]. Azari et al. investigated the use of magnetic nanotube carbon adsorbents to remove nitrate from aqueous media. The results revealed that the optimal conditions of the variables were pH equal to 3, contact time 60 min, stirring speed 200 rpm, and 1 g adsorbent per liter [35].

Jalili et al. used the UV/ZnO nanophotocatalytic process for phenol decomposition. The results showed an inverse relationship between phenol removal efficiency and pH increase in the UV/ZnO nanophotocatalytic process.

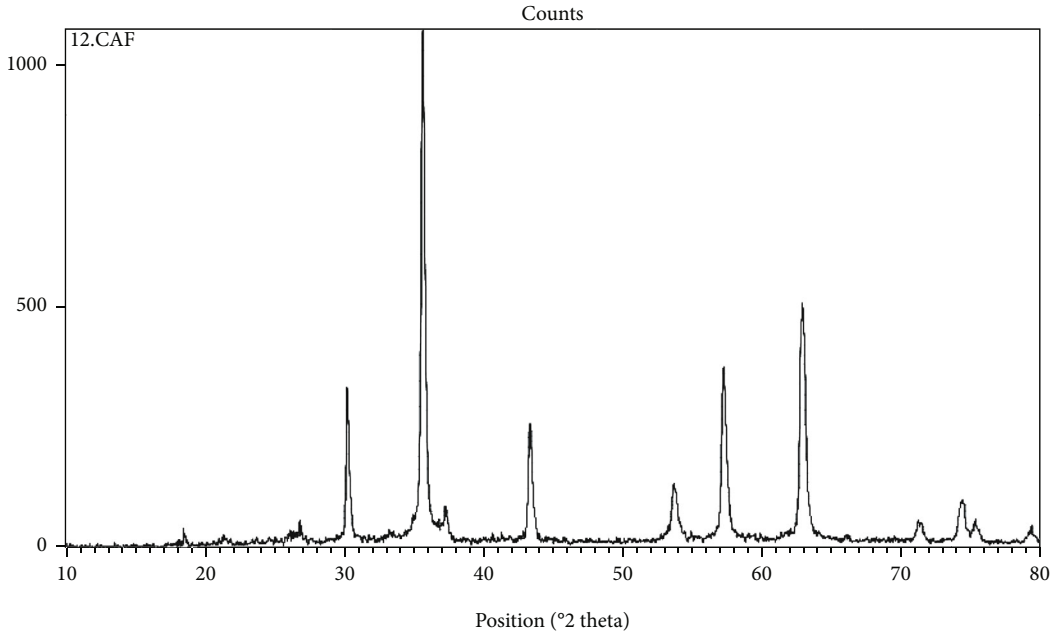

Figure 2: X-ray diffraction spectrum of Fe_3O_4 nanoparticles.

Optimal conditions in the UV/ZnO nanocatalytic process were 10 mg/L, contact time of 30 min, and pH = 5. Finally, according to this study, the UV/ZnO nanophotocatalytic process was an effective method for removing phenol from an aqueous solution [36]. In the other study, Ahmadi et al. used a magnetic zeolite nanocomposite prepared by coprecipitation to adsorb dimethyl phthalate (DMP). Also, the behavior of adsorption kinetics studies was consistent with the quasi-second-order kinetic model [37].

Azari et al. evaluated the ultrasonic dispersed solid-phase magnetic adsorption method with a high-performance liquid chromatographic system to remove diethyl phthalate (DEP). The primary interaction of parameters such as pH (3-11), adsorbent dose (0.10–0.50 g L^{-1}), ultrasound time (1–5 min), and DEP concentration (5–10 mg/L) was considered. The results showed that MGO has outstanding potential as an adsorbent to remove phthalates from contaminated water [38]. Ferrous nanoparticles are studied due to their abundance, cost-effectiveness, nontoxicity, fast reaction, high ability, and efficiency in decomposing pollutants such as organic matters [37–39]. Nanoparticles' specific surface increases with decreasing particle size, which some studies have suggested the successful use of iron nanoparticles in removing some antibiotics such as amoxicillin, ampicillin, and metronidazole [35–41].

The present study optimized the influential variables in removing CIP antibiotics using the Box–Behnken design (BBD) method based on the response surface methodology (RSM). In this study, magnetite nanoparticles such as adsorbents have been investigated, and the characterization of nanoparticles synthesized using techniques such as X-ray diffraction (XRD), scanning electron microscopy (SEM), and Fourier transform spectroscopy (FT-IR) was determined.

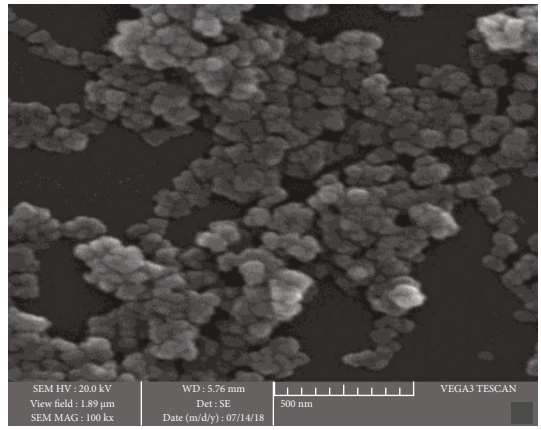

Figure 3: SEM images of Fe_3O_4 nanoparticles.

2. Materials and Methods

The materials used, such as CIP powders ($C_{17}H_{18}FN_3O_3$, 98% in purity) were purchased from Temad Pharmaceutical and Nanosany Companies, Iran. Ferric chloride hexahydrate and Ferrous chloride tetrahydrate ($FeCl_3.6H_2O$, $FeCl_2.4H_2O$), sulfuric acid (H_2SO_4), sodium hydroxide (NaOH), ammonia solution (NH_3, 25%), and nitric acid (HNO_3) were prepared from Merck company.

2.1. Experimental Procedures. Experimental design is a method for conducting a systematic set of experiments to obtain reliable and appropriate results based on a limited number of observations [42–44]. Optimization techniques may be used to identify the optimal values for variables and investigate the effect of optimized parameters on the response. The main tools in this field are divided into two groups of

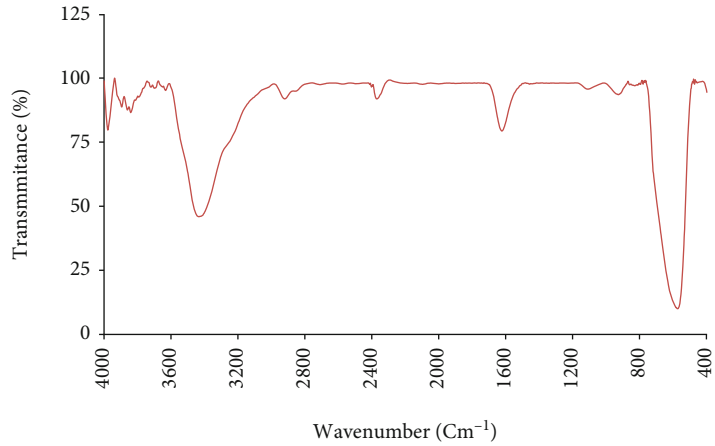

Figure 4: FT-IR spectrum of Fe_3O_4 nanoparticles.

experiment design and analysis tools. In the experimental design, there are methods such as the full factorial method and Latin square-based method. The experimental analysis, including the analysis of variance (ANOVA), its derivatives, and regression analysis are the essential tools. The flowchart proposed for optimization of CIP removal by the synthesis of magnetite nanoparticles is presented in Figure 1.

RSM is one of the most powerful statistical tools, which is helpful for optimizing influential variables in various processes, and it is widely used for designing experiments [45–47]. Examination of the effect of different variables and their interaction on the response of different experimental design methods should be done systematically based on the number of experiments. The most important designs of optimization experiments include full three-level factorial design (FFD), BBD, and central composite design (CCD). In the FFD method, the number of experiments can be obtained with n^k, in which k is all variables that have an equal number of levels n and the level of the variables included are +1, 0, and -1 (maximum, mean, and minimum), respectively. The number of experiments executions is associated with an increase in the number of variables and levels. Time consumption and high cost are the main disadvantages of this method. The nature of FFD means that its results can be a good reference for discussing the performance of other designs. In the BBD design, there are three imperfect levels of factorial design (3^k). It is a quadratic or (approximately rotatable) quadratic spherical design. A practical advantage of the common use of the BBD is an economical design in industrial research. Its feasibility is possible with a limited number of experiments, requiring only three levels for each factor. In CCD experimental design, the number of experiments (N) required for this method was defined as $N = n_0 + 2^K + 2K$, in which K was the number of variables and n_0 was the number of central points as well as; in the CCD method, each variable is divided into five different levels and three different levels in the BBD method [47, 48].

In the BBD method, the variables are in three levels of high (+1), medium (0), and low (-1) with five central repetition points (to estimate the percentage error of the sum of squares), with a total of 17 experiments, designed by the Design-Expert software (DX7). The number of experiments required for the model was determined from Equation (1):

$$N = 2K(K-1) + C_0, \tag{1}$$

where N is the number of experimental specimens, K is the number of factors (variables), and C_0 is the number of center points. The model was used for cross-over interaction to evaluate data, and experiments were performed randomly to avoid systemic error [44–49]. Coefficients were examined using ANOVA, and a P value of less than 0.05 was considered a significant level. Using this statistical model is due to the high cost of nanoparticles, reducing the sample volume and giving a quadratic equation [45, 50]. In this study, three parameters, namely, initial concentration of CIP, adsorbent dose, and pH at a contact time of 80 min, were investigated. The practical factors and their study levels in removing the CIP antibiotics are presented in Table 1.

In this method, the experiments are performed in turn and according to the values provided for the design of the BBD in Table 1. To perform each sample, a specific concentration of an antibiotic solution is mixed with a certain amount of adsorbent in a pH and specified contact time. Finally, the nanoparticles are separated with centrifugation and external magnetic, so the concentration of antibiotics remaining in the solution is measured with a UV-Vis spectrophotometer. Fit analysis was carried out, and the accuracy and correctness of the obtained results were investigated. For this purpose, $R(\%)$ which is the percentage of antibiotics removal was considered the response variable according to Equation (2).

$$R(\%) = \frac{C_{0-}C_t}{C_0} \times 100. \tag{2}$$

The CIP removal efficiency was evaluated through (Equation (2)), the $(C_{0-}C_t)/C_0$ ratio with C_0 and C_t representing the initial and final concentrations of CIP in solution (ppm), respectively.

Table 2: The results of the Box-Behnken experimental design (BBD).

Run	Block	*A*: CIP (mg/L)	*B*: adsorbent dose (mg)	*C*: pH (-)	CIP removal (%)
1	Block 1	35.00	40.00	4.00	68.24
2	Block 1	57.50	40.00	7.00	64.50
3	Block 1	35.00	60.00	7.00	73.11
4	Block 1	57.50	40.00	7.00	68.21
5	Block 1	57.50	20.00	10.00	52.22
6	Block 1	80.00	60.00	7.00	65.32
7	Block 1	57.50	40.00	7.00	65.42
8	Block 1	80.00	40.00	10.00	48.35
9	Block 1	57.50	40.00	7.00	68.01
10	Block 1	80.00	20.00	7.00	60.32
11	Block 1	80.00	40.00	4.00	59.21
12	Block 1	57.50	60.00	4.00	74.20
13	Block 1	35.00	40.00	10.00	61.23
14	Block 1	57.50	40.00	7.00	67.32
15	Block 1	57.50	20.00	4.00	70.01
16	Block 1	57.50	60.00	10.00	62.01
17	Block 1	35.00	20.00	7.00	70.12

Table 3: Results of analysis of variance (ANOVA).

Source	Sum of Squares	df	Mean Square	*F* Value	*P* value *Prob* > *F*	
Model	717.57	9	79.73	15.50	0.0008	Significant
A: CIP (mg/L)	195.03	1	195.03	37.91	0.0005	
B: Fe_3O_4	60.34	1	60.34	11.73	0.0111	
C: time (min)	286.20	1	286.20	55.64	0.0001	
AB	1.01	1	1.01	0.20	0.6711	
AC	3.71	1	3.71	0.72	0.4241	
BC	7.84	1	7.84	1.52	0.2568	
A^2	24.53	1	24.53	4.77	0.0653	
B^2	36.37	1	36.37	7.07	0.0325	
C^2	106.15	1	106.15	20.64	0.0027	
Residual	36.01	7	5.14			
Lack of fit	25.15	3	8.38	3.09	0.1523	Not significant
Pure error	10.86	4	2.71			
Cor total	753.58	16				

Std.Dev = 2.27. R^2 = 0.9522. Adj R^2 = 0.8908. CV% = 3.51. Pred R^2 = 0.4435. PRESS = 419.36. Adeq precision = 15.53.

3. Results and Discussion

3.1. Synthesis of Magnetite (Fe_3O_4) Nanoparticles. The relevant nanoparticles were synthesized by the coprecipitation method. First, 1.625 g of $FeCl_2.4H_2O$ with 4.43 g of $FeCl_3.6H_2O$ was mixed with 320 mL of deionized water by a magnetic stirrer for one hour at 80°C. Then, after the end of the reaction time, 12.5 mL of ammonia (NH_3, 25%) was added slowly to the solution of the first part at 80°C, so a black precipitate was formed at the bottom of the Erlenmeyer flask, representing nanoparticles. After extraction, the stirrer is removed, and it is slowly washed three times with ethanol and distilled water and filtered with a vacuum pump. The precipitate was finally dried under a vacuum for 24 hours. Figures 2–4 show the results of the analysis of XRD, SEM, and FT-IR nanoparticles, respectively.

The obtained nanoparticles were examined using XRD to analyze the structure and composition of the particles. The phase-detection and crystalline properties were determined by X-ray diffraction (XRD) using a Siemens D5000 diffraction gauge. Scattering was obtained using Cu-Kα radiation ($\lambda = 1.5406\,\lambda$) in the range of $10^\circ < 2\theta^\circ < 80^\circ$ with steps

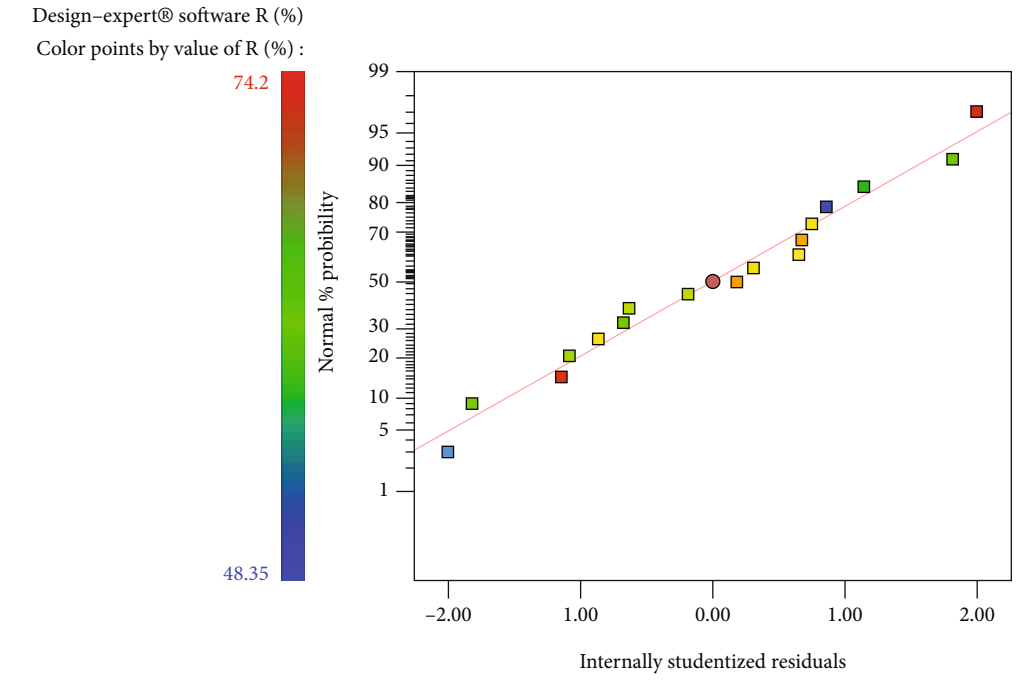

(a)

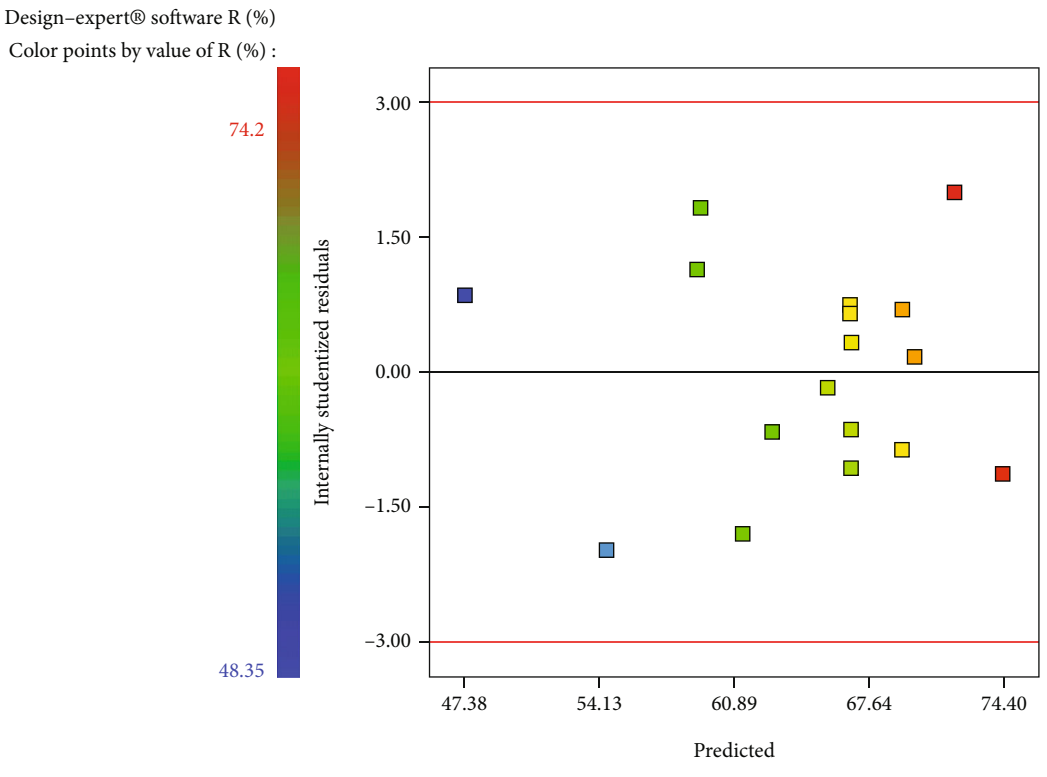

(b)

Figure 5: Continued.

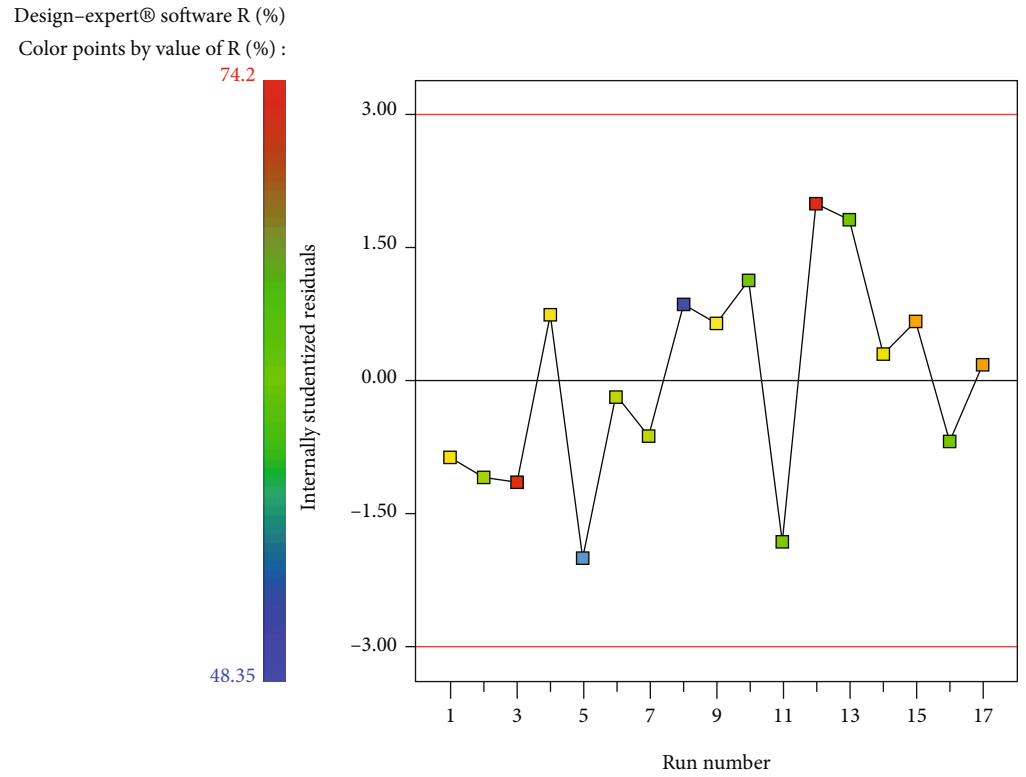

(c)

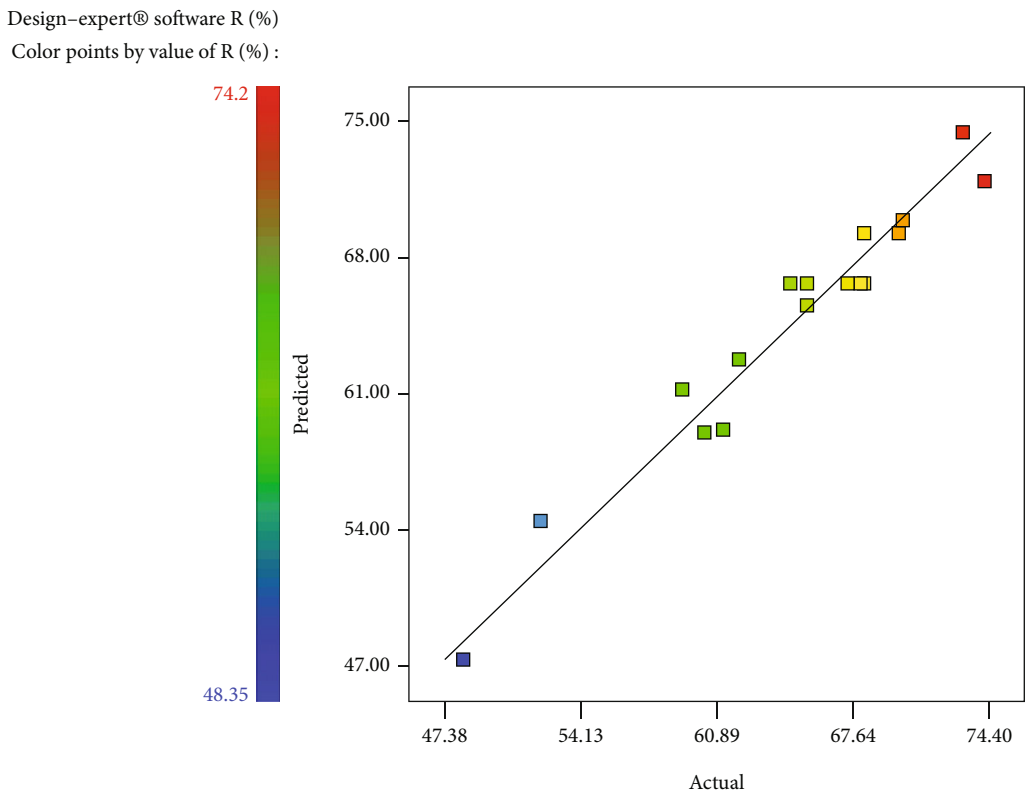

(d)

Figure 5: (a) Normal probability of student residuals. (b) Residuals versus predicted. (c) Residuals versus run number. (d) Measured values versus predicted values.

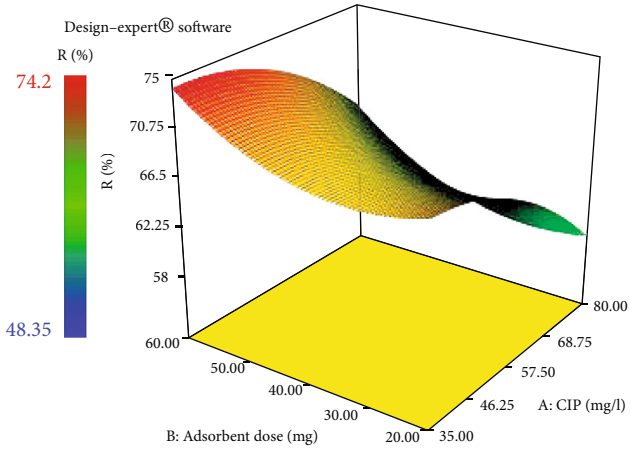

X1 = A: CIP (mg/l)
X2 = B: Adsorbent dose (mg)

Actual factor
C: pH = 7.00

(a)

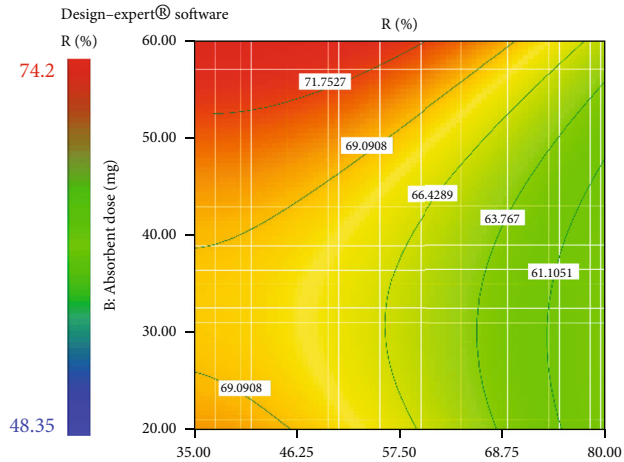

X1 = A: CIP (mg/l)
X2 = B: Absorbent dose (mg)

Actual factor
C: pH = 7.00

(b)

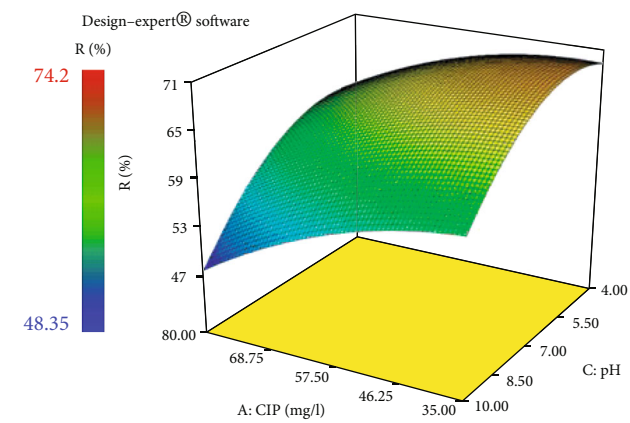

X1 = A: CIP (mg/l)
X2 = C: pH

Actual factor
B: Catalyst dose (mg/l) = 40.00

(c)

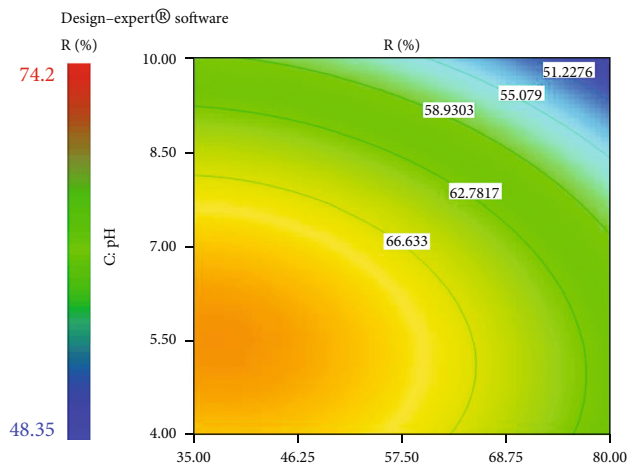

X1 = A: CIP (mg/l)
X2 = C: pH

Actual factor
B: Catalyst dose (mg) 40.0

(d)

Figure 6: Continued.

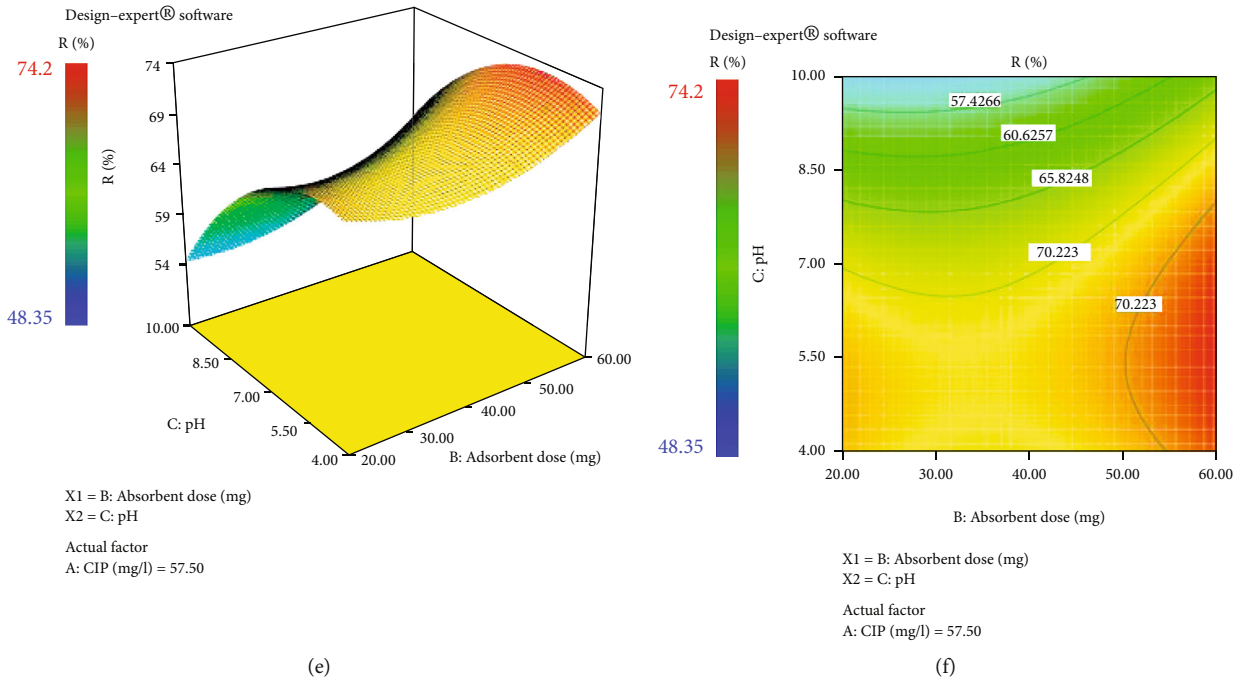

FIGURE 6: Response surface plots (3D) and contour plots (2D): (a, b) interaction between adsorbent dose and initial concentration of CIP (mg/L), (c, d) interaction between initial concentration of CIP (mg/L) and pH, and (e, f) interaction between adsorbent dose and pH.

of 0.02° and an achievement time of 1.0 s in steps. As shown in Figure 2, phase analysis results for magnetite Fe_3O_4 particles have reasonably good compatibility between the peaks that become seen in the sample with the literature [51–53].

The shown angles for the peaks in the sample at $2\theta =$ 30, 35.22, 43.35, 53.68, 57, 62.79, and 71.38 deg which correspond to the crystal planes 220, 311, 400, 422, 511, 440, and 535, respectively, were in accordance with the standard peaks of magnetite with a cubic face structure.

The properties of Fe_3O_4 nanoparticles were determined using various devices to study the shape, the average diameter of the particles, and the surface details of the nanoparticles that were taken by SEM Figure 3.

The image of the nanoparticles synthesized by the coprecipitation taken with SEM showed that the nanoparticles produced had the form of clusters of cohesive spherical particles that have irregular shapes and were more or less uniform and had a balanced surface. As can be seen in Figure 3, the diameter of the nanoparticles is in the range of 20-48 nm and 34 nm on average which is in the expected range. Based on the empirical classification given by IUPAC, particles with a diameter of $2 < d < 50$ nm may be classified as mesopore particles [54, 55]. FT-IR spectroscopy was applied to study the functional groups on the surface of nanoparticles, which is illustrated in Figure 4.

FT-IR is a crucial method for investigating chemical bond groups and functional groups on the surface of nanosorbent particles [51]. In this study, FT-IR was used to investigate the chemical bonds and levels of nanoparticles and the interactions that occurred at these levels during adsorption on the Fe_3O_4 surface [40]. The FT-IR spectra of Fe_3O_4 nanoparticles in the range bands at 400 cm^{-1} to 4000 cm^{-1} have been prepared and indicate that in this spectrum the functional groups in the frequency of 572 cm^{-1} which are related to the formation of the band the Fe-O and generally peak wavelength of bands 572 cm^{-1}, 1622 cm^{-1}, and 3420 cm^{-1} attributed to the tensile and flexural vibration of bond O-Fe, absorption band C=C, and the O-H bond in water adsorption (or carboxylic groups), respectively [52–56]. In this regard, the size of Fe_3O_4 particles decreases to the nanoscale, the constant bond strength will increase, as a large number of bonds of surface atoms are broken as a result of the rearrangement of unstable electrons on the particle surface.

3.2. Experimental Design and Optimization Using BBD. Based on the experimental design results and statistical analysis performed on the response, the use of a quadratic statistical model was evaluated. The model results obtained by experimental design software are shown in Equation (3).

$$\begin{aligned}\text{CIP removal}(R\%) = {} & +66.69 - 4.94\,A + 2.75\,B - 5.98\,C \\ & + 0.50\,AB - 0.96\,AC + 1.40\,BC \\ & - 2.41\,A^2 + 2.94\,B^2 - 5.02\,C^2.\end{aligned} \quad (3)$$

A positive (negative) sign indicates that the variables have a direct (inverse) effect on the target. Tables 2 and 3 indicate the results of BBD experiments and ANOVA, respectively.

According to Table 3, the F value of the model is equal to 15.50, and the P value (<0.0001) variables, lack of fit of the model, and other coefficients achieved from the model indicate the significance of the proposed model for CIP removal using nanoparticles. Also, according to the results in Figure 5 ((a) normal probability of student residuals, (b)

Table 4: Summary of studies performed using nanotechnology to the removal of different types of antibiotics.

Treatment parameters	Antibiotic compound	Main findings	References
pH values (3–11); catalyst dosages (250–750 mg/L); reaction times (30–90 min); at an ozonation rate of 200 mg/h	Amoxicillin	The following results were obtained under optimal conditions: pH = 11, catalyst dose = 500 mg/L, reaction time = 90 min, and the amoxicillin degradation efficiency = 78.7%	[57]
Vanadium dioxide (0.49 g/L); pH 7; ~58.3 min	Ciprofloxacin	The adsorption capacity of ciprofloxacin was achieved using belt-like nanostructured vanadium diox by 102.2 mg/g nanoVO2	[58]
Silver@reduced graphene oxide	Sulfamethoxazole	The results showed that 0.007 g of regenerated silver graphene oxide nanocomposite @ at pH = 5 after 3600 s contact time could remove 88% (188.57 mg/g) of sulfamethoxazole from 0.05 dm3 solution (initial concentration 30 mg/dm3)	[59]
pH (2-9); temperature (°C) (21-40); antibiotic volume (mL) (1-5)	Piperacillin tazobactam sulfamethoxazole tetracycline trimethoprim ampicillin and erythromycin	The results showed that Fe_3O_4 nanoparticles synthesized with different extracts showed high removal (more than 90%) of the studied antibiotics with the exception of SUL and TRI	[60]

residuals versus predicted, (c) residuals versus run number, and (d) measured values versus predicted values), the results of the achieved model were satisfied. The residual values indicate the normal distribution of the applied variables near the mean values. Therefore, one of the proposed models for predicting CIP removal efficiency is the regression model. Based on this model, the graph of the measured values provides a good agreement with the predicted values.

Also, in Figure 6, response surface plots (3D) and contour plots (2D) showed the effects of variables, the interaction between adsorbent dosage and initial concentration of CIP (mg/L) (Figures 6(a) and 6(b)), the interaction between initial concentration of CIP (mg/L) and pH (Figures 6(c) and 6(d)), and the interaction between adsorbent dose and pH (Figures 6(e) and 6(f)) vs. response, respectively. According to Figure 6, from the three-dimensional response surfaces and contours related to the variables, it can be concluded that in Figures 6(a) and 6(b), with the increasing the amount of adsorbent dose up to 50 mg and decreasing the initial concentration of antibiotics less than 50 mg/L, the highest percentage of removal was observed. Also, in Figures 6(c) and 6(d), with a decreased pH of less than 5.5 and the initial concentration of antibiotics less than 46 mg/L, the highest percentage of removal was observed. In Figures 6(e) and 6(f), the highest removal percentage was observed by increasing the amount of adsorbent dose ≅ 55 mg and decreasing the pH to less than 5.5. A summary of studies performed using nanotechnology to remove different types of antibiotics is shown in Table 4.

4. Conclusion

Due to the simultaneous effect of variables such as initial antibiotic concentration, adsorbent dosage, pH, and contact time, nanotechnology can be more effective as adsorbents for the removal of various types of contaminants than other methods. The results of XRD showed that the angles for the peaks at $2\theta = 30, 35.22, 43.35, 53.68, 57, 62.79$, and 71.38 deg, which corresponded to the crystal planes 220, 311, 400, 422, 511, 440, and 535, respectively, were in accordance with the standard peaks of magnetite with a cubic face structure. The results of SEM showed that the diameter of the nanoparticles is in the range of 20-48 nm and 34 nm in average which is in the expected range.

The results of the experimental data with the predicted model had good accuracy ($R^2 = 0.95$, $R^2\text{Adj} = 0.89$). After evaluating the desirability of the results of the analysis of variance, the optimal values of the variables were assessed, and several optimal points with high desirability were suggested. The obtained results showed that the CIP removal efficiency was (74.44%) under optimum operation parameters with the initial concentration of CIP 44.15 (mg/L), adsorbent dose of 59.6 (mg), pH ≅ 5, and contact time of 80 min. It was found that the effect of pH and nanoparticle dose has a significant role in the removal of CIP. The above-mentioned results confirm the suitability of using magnetic nanoparticles in wastewater treatment applications. Recently, research teams have been considering increasing the capabilities of nanoparticles and the possibility of using modified magnetite nanoparticles to study the removal of various pollutants.

Data Availability

The data used to support the findings of this study are included within the article.

Conflicts of Interest

The author declares that they have no conflicts of interest.

Acknowledgments

The author thanks the Temad Pharmaceutical and Nanosany Companies, for providing the drugs.

References

[1] M. Salari, E. Teymouri, and Z. Nassaj, "Application of an artificial neural network model for estimating of water quality parameters in the Karun River, Iran," *Journal of Environmental Treatment Techniques*, vol. 9, no. 4, pp. 720–727, 2021.

[2] M. Salari, M. Hosseini Kheirabad, M. Ehteshami, and S. N. Moaddeli, "Modeling of groundwater quality for drinking and agricultural purpose: a case study in Kahorestan plain," *Journal of Environmental Treatment Techniques*, vol. 8, no. 1, pp. 346–352, 2020.

[3] E. Salami, M. Salari, S. N. Sheibani, M. H. Kheirabad, and E. Teymouri, "Dataset on the assessments the rate of changing of dissolved oxygen and temperature of surface water, case study: California, USA," *Journal of Environmental Treatment Techniques*, vol. 7, no. 3, pp. 843–852, 2020.

[4] M. Khorasani, M. Ehteshami, H. Ghadimi, and M. Salari, "Simulation and analysis of temporal changes of groundwater depth using time series modeling," *Modeling Earth Systems and Environment*, vol. 2, no. 2, 2016.

[5] M. Salari, E. S. Shahid, S. H. Afzali et al., "Quality assessment and artificial neural networks modeling for characterization of chemical and physical parameters of potable water," *Food and Chemical Toxicology*, vol. 118, pp. 212–219, 2018.

[6] Z. M. Avval, L. Malekpour, F. Raeisi et al., "Introduction of magnetic and supermagnetic nanoparticles in new approach of targeting drug delivery and cancer therapy application," *Drug Metabolism Reviews*, vol. 52, no. 1, pp. 157–184, 2020.

[7] H. Peng, B. Pan, M. Wu, Y. Liu, D. Zhang, and B. Xing, "Adsorption of ofloxacin and norfloxacin on carbon nanotubes: hydrophobicity-and structure-controlled process," *Journal of Hazardous Materials*, vol. 233, pp. 89–96, 2012.

[8] R. Wei, F. Ge, S. Huang, M. Chen, and R. Wang, "Occurrence of veterinary antibiotics in animal wastewater and surface water around farms in Jiangsu Province, China," *Chemosphere*, vol. 82, no. 10, pp. 1408–1414, 2011.

[9] E. Teymouri, S. F. Mousavi, H. Karami, S. Farzin, and M. H. Kheirabad, "Municipal wastewater pretreatment using porous concrete containing fine- grained mineral adsorbents," *Journal of Water Process Engineering*, vol. 36, article 101346, 2020.

[10] E. Teymouri, S. F. Mousavi, H. Karami, S. Farzin, and M. H. Kheirabad, "Reducing urban runoff pollution using porous concrete containing mineral adsorbents," *Journal of Environmental Treatment Techniques*, vol. 8, no. 1, pp. 429–436, 2020.

[11] N. M. Vieno, T. Tuhkanen, and L. Kronberg, "Analysis of neutral and basic pharmaceuticals in sewage treatment plants and in recipient rivers using solid phase extraction and liquid chromatography–tandem mass spectrometry detection," *Journal of Chromatography A*, vol. 1134, no. 1-2, pp. 101–111, 2006.

[12] L. J. Githinji, M. K. Musey, and R. O. Ankumah, "Evaluation of the fate of ciprofloxacin and amoxicillin in domestic wastewater," *Water, Air, & Soil Pollution*, vol. 219, no. 1, pp. 191–201, 2011.

[13] S. P. Sun, H. Q. Guo, Q. Ke et al., "Degradation of antibiotic ciprofloxacin hydrochloride by photo-Fenton oxidation process," *Environmental Engineering Science*, vol. 26, no. 4, pp. 753–759, 2009.

[14] M. K. Musey, "Evaluation of the Fate of Ciprofloxacin and Amoxicillin in Simulated Domestic Waste Water," in *Doctoral dissertation*, Tuskegee University, 2006.

[15] A. Dirany, I. Sirés, N. Oturan, and M. A. Oturan, "Electrochemical abatement of the antibiotic sulfamethoxazole from water," *Chemosphere*, vol. 81, no. 5, pp. 594–602, 2010.

[16] L. Pretali, F. Maraschi, A. Cantalupi, A. Albini, and M. Sturini, "Water depollution and photo-detoxification by means of TiO_2: Fluoroquinolone antibiotics as a case study," *Catalysts*, vol. 10, no. 6, p. 628, 2020.

[17] H. Saini, S. Chhibber, and K. Harjai, "Azithromycin and ciprofloxacin: a possible synergistic combination against Pseudomonas aeruginosa biofilm-associated urinary tract infections," *International Journal of Antimicrobial Agents*, vol. 45, no. 4, pp. 359–367, 2015.

[18] T. G. Vasconcelos, D. M. Henriques, A. König, A. F. Martins, and K. Kümmerer, "Photo-degradation of the antimicrobial ciprofloxacin at high pH: identification and biodegradability assessment of the primary by-products," *Chemosphere*, vol. 76, no. 4, pp. 487–493, 2009.

[19] T. Garoma, S. K. Umamaheshwar, and A. Mumper, "Removal of sulfadiazine, sulfamethizole, sulfamethoxazole, and sulfathiazole from aqueous solution by ozonation," *Chemosphere*, vol. 79, no. 8, pp. 814–820, 2010.

[20] S. Chavoshan, M. Khodadadi, and N. Nasseh, "Photocatalytic degradation of penicillin G from simulated wastewater using the UV/ZnO process: isotherm and kinetic study," *Journal of Environmental Health Science and Engineering*, vol. 18, no. 1, pp. 107–117, 2020.

[21] A. S. Giri and A. K. Golder, "Ciprofloxacin degradation from aqueous solution by Fenton oxidation: reaction kinetics and degradation mechanisms," *Rsc Advances*, vol. 4, no. 13, pp. 6738–6745, 2014.

[22] J. P. Bavumiragira and H. Yin, "Fate and transport of pharmaceuticals in water systems: A processes review," *Science of The Total Environment*, vol. 823, p. 153635, 2022.

[23] G. R. Rakhshandehroo, M. Salari, and M. R. Nikoo, "Optimization of degradation of ciprofloxacin antibiotic and assessment of degradation products using full factorial experimental design by Fenton homogenous process," *Global NEST Journal*, vol. 20, no. 2, pp. 324–332, 2019.

[24] M. Salari, G. R. Rakhshandehroo, and M. R. Nikoo, "Multi-objective optimization of ciprofloxacin antibiotic removal from an aqueous phase with grey taguchi method," *Journal of Water and Health*, vol. 16, no. 4, pp. 530–541, 2018.

[25] M. Salari, G. R. Rakhshandehroo, and M. R. Nikoo, "Degradation of ciprofloxacin antibiotic by homogeneous Fenton oxidation: hybrid AHP-PROMETHEE method, optimization, biodegradability improvement and identification of oxidized by-products," *Chemosphere*, vol. 206, pp. 157–167, 2018.

[26] C. T. Wang, W. L. Chou, M. H. Chung, and Y. M. Kuo, "COD removal from real dyeing wastewater by electro-Fenton technology using an activated carbon fiber cathode," *Desalination*, vol. 253, no. 1-3, pp. 129–134, 2010.

[27] X. Xing, J. Feng, G. Lv et al., "Adsorption mechanism of ciprofloxacin from water by synthesized birnessite," *Advances in Materials Science and Engineering*, vol. 2015, Article ID 148423, 7 pages, 2015.

[28] M. Ahmaruzzaman, "Adsorption of phenolic compounds on low-cost adsorbents: a review," *Advances in Colloid and Interface Science*, vol. 143, no. 1-2, pp. 48–67, 2008.

[29] B. Crittenden and W. J. Thomas, "Adsorption technology and design," Elsevier, 1998.

[30] D. M. Ruthven, *Principles of adsorption and adsorption processes*, John Wiley & Sons, 1984.

[31] G. Sharma, A. Kumar, S. Sharma et al., "Fe_3O_4/ZnO/Si_3N_4 nanocomposite based photocatalyst for the degradation of dyes from aqueous solution," *Materials Letters*, vol. 278, article 128359, 2020.

[32] P. Dhiman, A. Kumar, M. Shekh et al., "Robust magnetic ZnO-Fe_2O_3 Z-scheme hetereojunctions with in-built metal-redox for high performance photo- degradation of sulfamethoxazole and electrochemical dopamine detection," *Environmental Research*, vol. 197, article 111074, 2021.

[33] A. Kumar, S. K. Sharma, A. Kumar et al., "High interfacial charge carrier separation in Fe_3O_4 modified $SrTiO_3$/$Bi_4O_5I_2$ robust magnetic nano-heterojunction for rapid photodegradation of diclofenac under simulated solar-light," *Journal of Cleaner Production*, vol. 315, article 128137, 2021.

[34] Y. Rashtbari, S. Hazrati, A. Azari, S. H. Afshin, M. Fazlzadeh, and M. Vosoughi, "A novel, eco-friendly and green synthesis of PPAC-ZnO and PPAC-nZVI nanocomposite using pomegranate peel: cephalexin adsorption experiments, mechanisms, isotherms and kinetics," *Advanced Powder Technology*, vol. 31, no. 4, pp. 1612–1623, 2020.

[35] A. Azari, A. A. Babaie, R. Rezaei-Kalantary, A. Esrafili, M. Moazzen, and B. Kakavandi, "Nitrate removal from aqueous solution by carbon nanotubes magnetized with nano zero-valent iron," *Journal of Mazandaran University of Medical Sciences*, vol. 23, no. 2, pp. 15–27, 2014.

[36] N. Davood Jalili, A. Azari, N. Mirzaei et al., "Parameters effecting on photocatalytic degradation of the phenol from aqueous solutions in the presence of ZnO nanocatalyst under irradiation of UV-C light," *Bulgarian Chemical Communications*, vol. 47, pp. 14–18, 2015.

[37] E. Ahmadi, B. Kakavandi, A. Azari et al., "The performance of mesoporous magnetite zeolite nanocomposite in removing dimethyl phthalate from aquatic environments," *Desalination and Water Treatment*, vol. 57, no. 57, pp. 27768–27782, 2016.

[38] A. Azari, M. H. Mahmoudian, M. Hazrati Niari et al., "Rapid and efficient ultrasonic assisted adsorption of diethyl phthalate onto $Fe^{II}Fe_2^{III}O_4$@GO: ANN-GA and RSM-DF modeling, isotherm, kinetic and mechanism study," *Microchemical Journal*, vol. 150, article 104144, 2019.

[39] A. Ghauch, T. Almuthanna, and A. Hala Abou, "Antibiotic removal from water: elimination of amoxicillin and ampicillin by microscale and nanoscale iron particles," *Environmental Pollution*, vol. 157, no. 5, pp. 1626–1635, 2009.

[40] J. Yang, X. Wang, M. Zhu, H. Liu, and J. Ma, "Investigation of PAA/PVDF-NZVI hybrids for metronidazole removal: synthesis, characterization, and reactivity characteristics," *Journal of Hazardous Materials*, vol. 264, pp. 269–277, 2014.

[41] T. G. Vasconcelos, K. Kümmerer, D. M. Henriques, and A. F. Martins, "Ciprofloxacin in hospital effluent: degradation by ozone and photoprocesses," *Journal of Hazardous Materials*, vol. 169, no. 1-3, pp. 1154–1158, 2009.

[42] M. Salari, G. R. Rakhshandehroo, and M. R. Nikoo, "Developing multi-criteria decision analysis and Taguchi method to optimize ciprofloxacin removal from aqueous phase," *Environmental Engineering & Management Journal (EEMJ)*, vol. 18, no. 7, pp. 1543–1552, 2019.

[43] M. Salari, G. R. Rakhshandehroo, M. R. Nikoo, M. M. Zerafat, and M. G. Mooselu, "Optimal degradation of ciprofloxacin in a heterogeneous Fenton-like process using (δ-FeOOH)/MWCNTs nanocomposite," *Environmental Technology & Innovation*, vol. 23, article 101625, 2021.

[44] M. Shoorangiz, M. R. Nikoo, M. Salari, G. R. Rakhshandehroo, and M. Sadegh, "Optimized electro-Fenton process with sacrificial stainless steel anode for degradation/mineralization of ciprofloxacin," *Process Safety and Environmental Protection*, vol. 132, pp. 340–350, 2019.

[45] A. R. Khataee, M. Safarpour, M. Zarei, and S. Aber, "Combined heterogeneous and homogeneous photodegradation of a dye using immobilized TiO_2 nanophotocatalyst and modified graphite electrode with carbon nanotubes," *Journal of Molecular Catalysis A: Chemical*, vol. 363, pp. 58–68, 2012.

[46] C. L. Ngan, M. Basri, F. F. Lye et al., "Comparison of Box-Behnken and central composite designs in optimization of fullerene loaded palm-based nano-emulsions for cosmeceutical application," *Industrial Crops and Products*, vol. 59, pp. 309–317, 2014.

[47] A. L. Müller, J. A. de Oliveira, O. D. Prestes, M. B. Adaime, and R. Zanella, "Design of experiments and method development," in *Solid-Phase Extraction*, pp. 589–608, Elsevier, 2020.

[48] R. Srimanta, J. A. Lalman, and B. Nihar, "Using the box-Benkhen technique to statistically model phenol photocatalytic degradation by titanium dioxide nanoparticles," *Chemical Engineering Journal*, vol. 150, no. 1, pp. 15–24, 2009.

[49] J. S. Ye, J. Liu, H. S. Ou, and L. L. Wang, "Degradation of ciprofloxacin by 280 nm ultraviolet-activated persulfate: degradation pathway and intermediate impact on proteome of Escherichia coli," *Chemosphere*, vol. 165, pp. 311–319, 2016.

[50] N. Singh, S. Riyajuddin, K. Ghosh, S. K. Mehta, and A. Dan, "Chitosan-graphene oxide hydrogels with embedded magnetic iron oxide nanoparticles for dye removal," *ACS Applied Nano Materials*, vol. 2, no. 11, pp. 7379–7392, 2019.

[51] M. M. Zaman, M. A. Karal, M. N. Khan et al., "Eco-friendly synthesis of Fe_3O_4 nanoparticles based on natural stabilizers and their antibacterial applications," *Chemistry Select*, vol. 4, no. 27, pp. 7824–7831, 2019.

[52] V. R. Akshay, M. Vasundhara, and M. Arumugam, "Biosynthesis of multiphase iron nanoparticles using *Syzygium aromaticum* and their magnetic properties," *Colloids and Surfaces A: Physicochemical and Engineering Aspects*, vol. 603, article 125241, 2020.

[53] M. Ehteshami, Z. Hamidreza, M. Salari, and E. Teymouri, "Mespilus germanica (MG) and Tribulus terrestris (TT) used as biosorbents for Lead removal from aqueous solutions: adsorption kinetics and mechanisms," *Advances in Materials Science and Engineering*, vol. 2021, Article ID 8436632, 13 pages, 2021.

[54] M. Salari and H. Hosseini, "Application of nanoparticle technology in water and wastewater treatment (overview)," *Advances in Applied Nano Bio-Technologies*, vol. 2, no. 4, pp. 86–91, 2021.

[55] B. Kakavandi, A. Takdastan, N. Jaafarzadeh, M. Azizi, A. Mirzaei, and A. Azari, "Application of Fe_3O_4@C catalyzing heterogeneous UV-Fenton system for tetracycline removal with a focus on optimization by a response surface method," *Journal of Photochemistry and Photobiology A: Chemistry*, vol. 314, pp. 178–188, 2016.

[56] M. G. Lak, M. R. Sabour, A. Amiri, and O. Rabbani, "Application of quadratic regression model for Fenton treatment of municipal landfill leachate," *Waste Management*, vol. 32, no. 10, pp. 1895–1902, 2012.

[57] E. Norabadi, A. Hossein Panahi, R. Ghanbari, A. Meshkinian, H. Kamani, and S. D. Ashrafi, "Optimizing the parameters of amoxicillin removal in a photocatalysis/ozonation process using Box–Behnken response surface methodology," *Desalination and Water Treatment*, vol. 192, pp. 234–240, 2020.

[58] N. T. Nezhad, M. Shams, A. Dehghan et al., "Vanadium dioxide nanoparticles as a promising sorbent for controlled removal of waterborne fluoroquinolone ciprofloxacin," *Materials Chemistry and Physics*, vol. 259, article 123993, 2021.

[59] M. Keshvardoostchokami, S. Rasooli, A. Zamani, A. Parizanganeh, and F. Piri, "Removal of sulfamethoxazole antibiotic from aqueous solutions by silver@ reduced graphene oxide nanocomposite," *Environmental Monitoring and Assessment*, vol. 191, no. 6, pp. 1–16, 2019.

[60] M. Stan, I. Lung, M. L. Soran et al., "Removal of antibiotics from aqueous solutions by green synthesized magnetite nanoparticles with selected agro-waste extracts," *Process Safety and Environmental Protection*, vol. 107, pp. 357–372, 2017.